Transition dipole orientations in the early photolysis intermediates of rhodopsin

J. W. Lewis, C. M. Einterz, S. J. Hug, and D. S. Kliger
Division of Natural Sciences, University of California, Santa Cruz, California 95064

ABSTRACT The linear dichroism spectrum of rhodopsin in sonicated bovine disk membranes was measured 30, 60, 170, and 600 ns after room temperature photolysis with a linearly polarized, 7-ns laser pulse (λ = 355 or 477 nm). A global exponential fitting procedure based on singular value decomposition was used to fit the linear dichroism data to two exponential processes which differed spectrally from one another and whose lifetimes were 42 ± 7 ns and 225 ± 40 ns. These results are interpreted in terms of a sequential model where bathorhodopsin (BATHO, λ_{max} = 543 nm) decays toward equilibrium with a blue shifted intermediate (BSI, λ_{max} = 478 nm). BSI then decays to lumirhodopsin (LUMI, λ_{max} = 492 nm). It has been suggested that two bathorhodopsins decay in parallel to their products. However, a Monte Carlo simulation of partial photolysis of solid-state visual pigment samples shows that one mechanism which creates populations of BATHO having different photolysis rates at 77 K may not be responsible for the two decay rates reported here at room temperature.

The angle between the *cis* band and 498-nm band transition dipoles of rhodopsin is determined to be 38°. The angles between both these transition dipoles and those of the long-wavelength bands of BATHO, BSI, and LUMI are also determined. It is shown that when BATHO is formed its transition dipole moves away from the original *cis* band transition dipole direction. The transition dipole then moves roughly twice as much towards the original *cis* band direction when BSI appears. Production of LUMI is associated with return of the transition dipole almost to the original orientation relative to the *cis* band, but with some displacement normal to the plane which contains the previous motions. The correlation between the λ_{max} of an intermediate and its transition dipole direction is discussed.

INTRODUCTION

Rhodopsin (RHO), a vertebrate visual pigment, passes through a number of distinct intermediate stages after the prosthetic chromophore, 11-*cis*-retinal, absorbs light. These intermediates have been principally characterized by their optical absorption spectra, and the sequence of reasonably well characterized photolysis intermediates observed after RHO photolysis is usually given by

$$\ldots \text{bathorhodopsin} \rightarrow \text{lumirhodopsin} \rightarrow \text{metarhodopsin I} \rightleftharpoons \text{metarhodopsin II} \ldots$$

Scheme 1

Although metarhodopsin II is followed by other stages, they are of secondary interest because it is the metarhodopsin II stage which activates a G-protein to transmit the visual message from the photoreceptor protein to its effector protein, a phosphodiesterase. Multiple exponential decays of metarhodopsin I have been observed (Stewart et al., 1977, Lewis et al., 1981), implying that a parallel set of intermediates might be present. Studies of the bathorhodopsin to lumirhodopsin process will help to clarify this issue by determining whether a parallel sequence of intermediates might extend to these earlier times as well. Further interest in understanding the early intermediates comes from the fact that hormone receptors are coupled to their effectors by G-proteins similar in nature to those of the visual system (Neer and Clapham, 1988). One model proposes that RHO is a hormone receptor analogue with 11-*cis*-retinal being a tethered, photoactivatible hormone analogue. This model implies that the RHO bleaching intermediates may be structural analogues of a similar sequence which occurs after hormone reception. In particular, a protein relaxation which is proposed to occur in the RHO bleaching sequence (Albeck et al., 1989; Einterz et al., 1990) on the 100-ns time scale at room temperature may disclose a similar process in hormone receptors. Such a process is more convenient to study in the visual system because the photoreceptor protein is far easier to purify and trigger than hormone receptor proteins.

Structural information on these membrane bound proteins is limited because of the lack of suitable crystals for x-ray diffraction studies. The transient nature of the RHO photolysis intermediates makes their characterization by x-ray even more of a challenge. In such a case, spectroscopy with polarized light can sometimes be used to gain structural information, especially about the important chromophore region. For a long chromophore

0006-3495/89/12/1101/11 $2.00

like retinal, the situation is particularly auspicious because the transition dipole of the longest wavelength band tends to coincide with the long axis of the molecule.

Previous work has shown that in RHO the transition dipole of the retinal molecule is inclined ~16° to the membrane plane (Liebman, 1962). This was determined from the linear dichroism of individual, oriented rod outer segments (ROS). Later, the angle between the transition dipole moments of RHO and bathorhodopsin were studied using the linear dichroism of oriented populations of bathorhodopsin created using a linearly polarized photolysis beam (Kawamura et al., 1979; Michel-Villaz et al., 1982). These previous linear dichroism measurements on bathorhodopsin have a number of limitations in common. First, they used large frog ROS, which resulted in a sieve effect (Michel-Villaz et al., 1982), making data analysis difficult. Second, only one of the two major chromophore bands was used for photoselection. Many interesting questions were left unanswered, such as how the bathorhodopsin transition dipole moment is oriented relative to the plane defined by the α (498 nm) and β (*cis* band, ~340 nm) band transition dipole moments. A final limitation of these previous linear dichroism measurements on the early photolysis intermediates is that they were conducted near liquid nitrogen temperature. This is significant because some intermediates important at room temperature may not develop observable concentrations at very low temperatures (Hug et al., 1990).

Careful study of bathorhodopsin decay at room temperature reveals two distinct spectral and kinetic processes, showing that scheme 1 is too simple (Einterz et al., 1987). Originally, these results were discussed in terms of a parallel model where any photon can produce one of two possible forms of bathorhodopsin, batho$_1$ or batho$_2$. The processes observed at room temperature were hypothesized to be the parallel decay of batho$_1$ and batho$_2$. This seemed plausible because at low temperatures two different forms of bathorhodopsin had previously been characterized (Sasaki et al., 1980). Later work using variable excitation power and wavelength in an attempt to perturb the relative amounts of the two bathorhodopsins was unable to alter the proportions produced at room temperature (Hug et al., 1990). This provoked interest in a sequential model as an explanation of the two processes. A simple sequential model did not fit temperature dependence data as well as a more complex sequential model with a reversible step between a single bathorhodopsin (BATHO) and a new blue-shifted intermediate (BSI). The initial processes in this scheme can be drawn as

$$\ldots \text{BATHO} \rightleftharpoons \text{BSI} \rightarrow \text{LUMI} \ldots,$$

Scheme 2

where lumirhodopsin (LUMI) is the unique product of BSI decay. Further support for scheme 2 comes from experiments conducted on the synthetic visual pigments 5,6-dihydroisorhodopsin (Albeck et al., 1989) and 13-demethylrhodopsin (Einterz et al., 1990).

In this paper we report time-resolved linear dichroism measurements made over a 1-μs period after linearly polarized photolysis of RHO in sonicated bovine disk membranes. Such photolysis produces an orientation distribution that is stable over the time scale of the measurement (rotational relaxation time for RHO in frog ROS membranes = 20 μs; Cone, 1972). This allows us to determine transition dipole moment directions for all the species in scheme 2 because at room temperature production of LUMI is complete within 1 μs, well before rotational diffusion becomes significant.

A distinct advantage of these experiments over low temperature measurements is that at room temperature the rate constants in scheme 2 are such that a significant concentration of BSI builds up. This is in contrast to the situation at low temperature where BSI decays far faster than it is formed (Hug et al., 1990). A further advantage of the measurements reported here is that 355 nm excitation was used as well as 477 nm excitation. This allows the orientation of the *cis* band transition dipole of RHO to be determined relative to the long wavelength transition dipoles of RHO, BATHO, BSI, and LUMI. If only one transition dipole moment of RHO is used for photoselection, the transition dipole moment of each photolysis intermediate is somewhat undetermined, lying anywhere in a cone at the observed angle relative to the photoselecting transition dipole moment direction. By using two RHO transition dipole moments for photoselection the transition dipole moments of the intermediates are more completely specified and can be uniquely specified with minimal additional information.

The photoselection results are useful in analyzing the different RHO photolysis schemes. In particular, the polarization data are found to favor a sequential model with reversible step (scheme 2) over the simple sequential model (scheme 1). More generally, the photoselection results are used to parameterize a Monte Carlo simulation of partial bleaching experiments which demonstrates a possible explanation for the different forms of bathorhodopsin observed at low-temperature. If it can be shown that the multiple low temperature forms of bathorhodopsin arise from the different orientations in the frozen sample and not from two chemically different bathorhodopsins, there is less reason to consider a parallel model at room temperature.

MATERIALS AND METHODS

Bovine ROS were prepared as previously described (Lewis et al., 1984). The ROS were washed free of extrinsic membrane proteins by three

cycles of centrifugation (model SS-34, Sorvall Instruments, Newton, CT; 17K rpm, 45 min) followed by resuspension in 1 mM EDTA solution (pH 7.0). The final pellet was resuspended in Tris buffer (10 mM Tris(hydroxymethyl)aminomethane, pH 7.0). The low salt conditions inhibit membrane aggregation to produce a disk suspension of RHO. For a typical experiment, 16 ml of disk suspension at 1 mg/ml RHO in Tris buffer was sonicated for ~5 minutes in an ice bath under argon with the microtip of a sonicator. To further reduce the extinction (apparent absorption due to light scattering) of the sample for optical experiments the sonicated material was then diluted to 0.33 mg/ml RHO using Tris buffer.

Time-resolved optical density measurements after laser excitation were performed at room temperature using an optical multichannel analyzer system described previously (Lewis et al., 1987). Absorbance was measured along a 1 cm pathlength, and photolysis took place perpendicular to this axis with pathlength 0.2 cm. Individual 24-μl samples, delivered by a stepper motor-driven syringe, were photolyzed by a vertically polarized, 7-ns pulse from either a Nd:YAG pumped dye laser (477 nm, 0.5 mJ/0.1 cm^2) or the third harmonic of a Nd:YAG laser (355 nm 2.0 mJ/0.1 cm^2). A Glan-Taylor linear polarizer in the monitoring beam allowed absorbance changes to be measured with light polarized either parallel ($\parallel$) or perpendicular ($\perp$) to the actinic polarization direction. Data presented here were based on the average of six different experiments.

Spectra to determine the amount of RHO bleached were not collected for most samples. It was originally assumed that the detergent added in that procedure (Albeck et al., 1989) would affect the bleach itself through its effect on light scattering. In the two cases where the average bleach was measured (at 355 nm excitation) the values obtained agreed well with the estimate obtained using the procedure described in Results. In any event, the appropriate bleach could at best only be determined in an average sense because rotational diffusion on the time scale of the bleach measurement (seconds) would erase the difference between bleach values measured using monitoring light polarized parallel and perpendicular to the actinic polarization direction.

The simulation of successive partial photolysis of a solid-state RHO sample was conducted using a Monte Carlo method implemented in TurboPascal 5.0. Advantages of Pascal for this type of calculation include the ability to define separate data types for vector representations in the laboratory and molecular coordinate systems. This particular implementation of Pascal also provided graphics routines which were useful in monitoring progress of the simulation. This program and sample input files are available from the authors on request. A typical run involving ~100 photolysis steps on 15,000 molecules required several hours of time on a microcomputer (80386 with 80387 mathematical coprocessor).

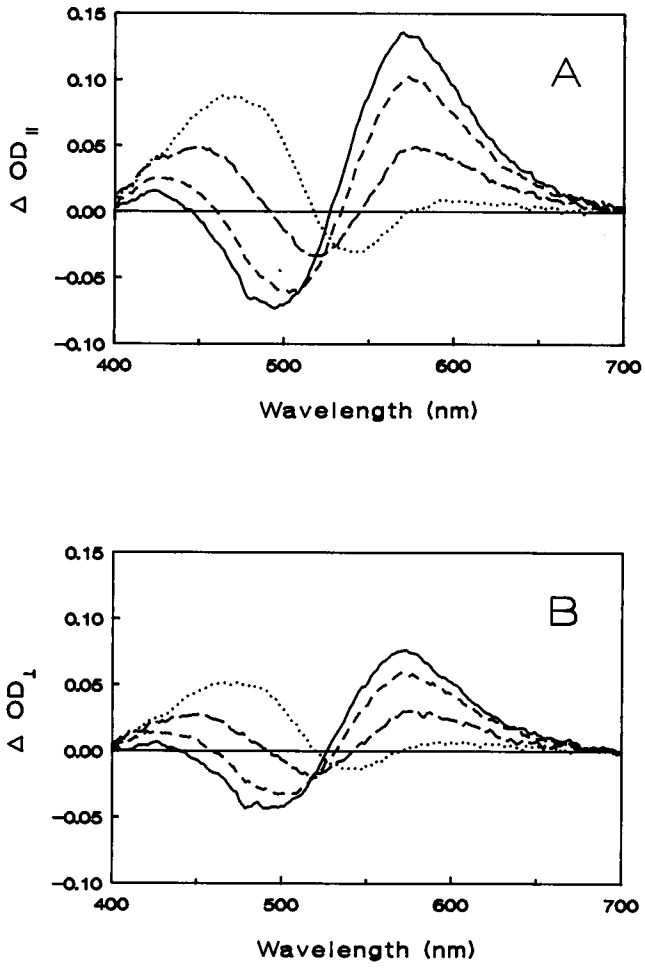

FIGURE 1 Difference spectra obtained at 30 ns ( ), 60 ns (- - -), 170 ns (———), and 600 ns (· · ·) after photolysis of sonicated disk suspensions of rhodopsin with 477 nm light. Spectra were collected using an optical multichannel analyzer with gate width of 10 ns. (*A*) Probe light was polarized parallel to the polarization direction of the actinic light. (*B*) Probe light was perpendicularly polarized.

RESULTS

The optical density changes observed at a series of times for probe beam polarizations parallel and perpendicular to the photolysis polarization direction are shown in Fig. 1 for 477 nm excitation and in Fig. 2 for 355 nm excitation. From this raw data it is clear that differences exist between the two photolysis wavelengths, particularly with respect to the polarization of the transient absorbance in the red portion of the spectrum at early times. This is expected given that the 355-nm excitation takes place in the chromophore *cis* band whose transition dipole moment should make a substantial angle with the transition dipole moment responsible for the main 498-nm band.

Data for a particular monitoring polarization and photolysis wavelength (e.g., those of Fig. 1 *A*) were fit to two exponential lifetimes using a global procedure based on singular value decomposition as described elsewhere (Hug et al., 1990). Because similar conditions prevailed for $\triangle OD_{\parallel}$ and $\triangle OD_{\perp}$ data sets at a particular photolysis wavelength, the lifetimes obtained from the $\triangle OD_{\parallel}$ and $\triangle OD_{\perp}$ data sets were averaged and then used to determine the independently time varying differences, the "*b* spectra." The average lifetimes were 38 ± 7 ns and 210 ± 40 ns for the 355-nm data and 46 ± 7 ns and 240 ± 40 ns for the 477-nm data. These values are in the range of those observed previously for detergent suspensions of

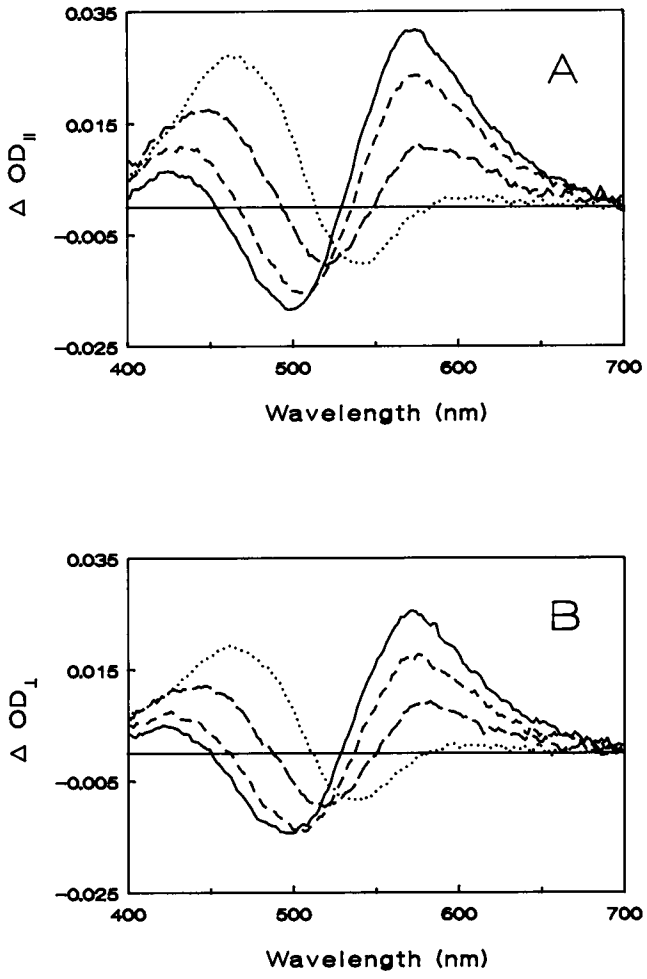

FIGURE 2 Difference spectra obtained at 30 ns ( ), 60 ns (- - -), 170 ns (———) and 600 ns (· · ·) after photolysis of sonicated disk suspensions of rhodopsin with 355 nm light. Spectra were collected using an optical multichannel analyzer with gate width of 10 ns. (*A*) Probe light was polarized parallel to the polarization direction of the actinic light. (*B*) Probe light was perpendicularly polarized.

RHO at room temperature (Hug et al., 1990). The fact that similar lifetimes are observed here compared to magic angle detergent samples is one demonstration that rotational diffusion is not occurring on the time scale of the reactions we are studying. Further evidence for this fact comes from our observation that the linear dichroism does not change over the period from 1 to 2 μs (data not shown). Because the previously reported exponential lifetime for the decay of rhodopsin dichroism in frog ROS at room temperature was ~4 μs, our observation confirms the suspicion that the membrane viscosity of warm-blooded vertebrates is as high or higher than the membrane viscosity of cold-blooded ones.

The difference spectra of BATHO, BSI, and LUMI were then calculated from the *b* spectra assuming a sequential decay model. These intermediate difference spectra represent the spectral change which would be observed when a given amount of RHO (the polarized bleach) is converted to BATHO, BSI, or LUMI. Two sets were calculated for each polarization, one for a simple sequential model and another for the sequential model with a reversible step between BATHO and BSI (K_{eq} = 1.4; Hug et al., 1990). The reason for calculating two sets of intermediate difference spectra was to test whether both models lead to equally plausible polarization consequences.

To calculate polarization ratios, $OD_{\parallel}/OD_{\perp}$, for the intermediates, we had to estimate the amount and polarization ratio of the bleached RHO. This polarized bleach information was needed because the polarization ratio is defined using absorbance ratios, not in terms of absorbance *difference* ratios. It is the polarization ratio, defined in this way, that is expected to be constant across a uniformly polarized band. For the reasons discussed in the experimental section, the average bleach and polarization ratio for RHO were not determined and estimates had to be made. This was done by choosing values that produced a polarized bleach that, when added to the BATHO intermediate difference spectrum, resulted in a constant polarization ratio across the BATHO absorbance band. The values chosen are shown in Table 1. For the reversible step model, the set of intermediate difference spectra obtained gave constant polarization ratios for the BSI and LUMI intermediates as well. The polarization ratios obtained for these intermediates are also given in Table 1. For the simple sequential model, the intermediate difference spectra obtained using this procedure resulted in a polarization ratio which varied across the BSI band. This was particularly pronounced for the 355 nm excitation data as shown in Fig. 3. Because the simple sequential model did not produce constant values, no polarization ratios are tabulated for it. In Table 1, the uncertainties associated with the polarization ratios were determined by calculating the root mean square deviation from the mean value over a 40 nm range centered on the tabulated λ_{max} for the intermediate. The uncertainty values reported here are 1.7 times the standard deviation of the mean (90% confidence limits).

TABLE 1 Results of SVD analysis of linear dichroism data

Photolysis Wavelength	477 nm	355 nm
Average Bleach (*OD*)	0.13	0.07
Polarization ratios ($OD_{\parallel}/OD_{\perp}$):		
RHO (498 nm)	1.87	1.28
BATHO (543 nm)	1.83 ± 0.01	1.21 ± 0.01
BSI (478 nm)	1.79 ± 0.03	1.50 ± 0.03
LUMI (492 nm)	1.782 ± 0.004	1.325 ± 0.004

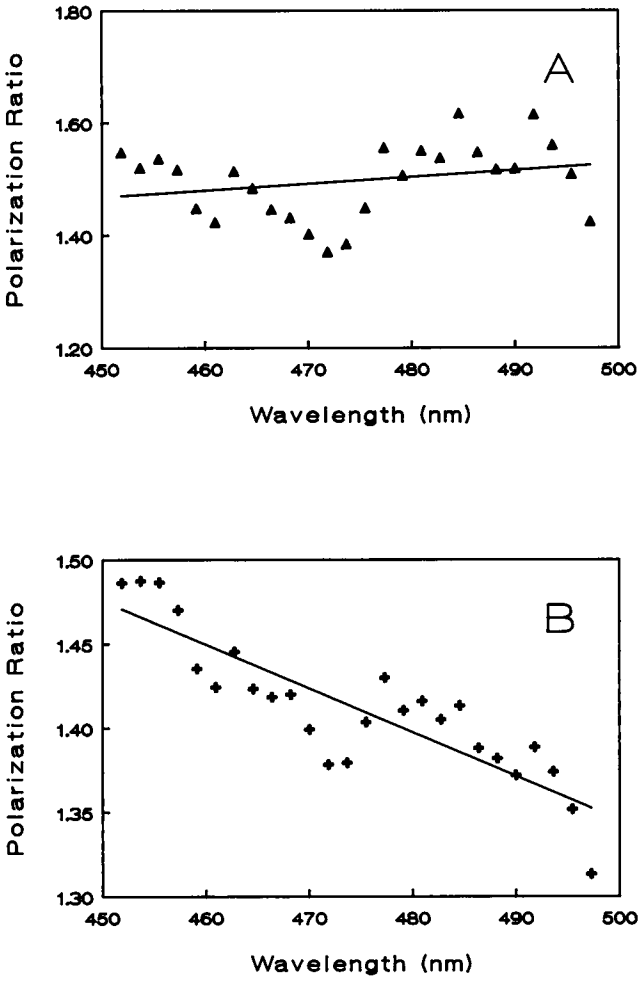

FIGURE 3 Polarization ratios obtained for the second (BSI) intermediate in the sequential models of the early photolysis products of rhodopsin. (*A*) Result of analysis using a sequential model including a reversible step between BATHO and BSI. When the data points were fit to a straight line as shown, the slope of the line was zero within experimental error. (*B*) Result of analysis using the simple sequential model with no equilibrium. When fit to a straight line as shown, the data points were found to have a slope whose magnitude was greater than could be accounted for by experimental uncertainty.

The value shown in Table 1 for the polarization ratio of RHO at 498 nm obtained using 477-nm excitation is less than that expected for photolysis of a molecule in a linearly polarized band when its absorbance is probed in that same band. The theoretical value of 3.0 is seldom achieved because of factors common in practical work, such as convergent probe or actinic beams, light scattering, and saturation of the absorber. Because many such factors are common in all the measurements described here, the value of 1.87 was used to normalize the results presented in Table 1 for computation of angles between transition dipole moments. The normalization in this case consists of multiplying the fractional part of the polarization ratio reported in the table by 2/0.87 and adding it back to the integer part. Thus ratios in the first column with values near 1.87, displaying little depolarization relative to the 498-nm band of RHO, result in normalized values near the ideal value of 3.0, whereas ratios near 1.0 which reflect little linear dichroism (and which consequently need little correction) will remain relatively unaffected near 1.0. An argument for this normalization is that it leads to reasonable agreement with previously measured transition dipole angles, and further, even if a quantitative error were introduced by it, the relative values of the angular changes would not be affected, leaving the qualitative conclusions unchanged.

The normalized value so obtained for RHO excited at 355 nm, 1.64 (obtained from the tabulated value 1.28), differs from 3.0 not because of the above-mentioned imperfections, but instead because of the angle between the transition dipole moments of the *cis* band and the 498 band of RHO. When 355-nm light is used, photolysis takes place in the *cis* band whereas the polarization ratio reported in Table 1 refers to wavelengths where the bleaching takes place near 498 nm (measurement of the polarization ratio at 355 nm was impossible because of the extinction of the sample due to scattered light). If a molecule has two transition dipole moments, say *a* and *b*, at an angle $\xi_{a,b}$ to one another and one of them is distributed with a probability proportional to $\cos^2\theta$ relative to some axis in the laboratory frame, the polarization ratio observed for the second moment is given by

$$\text{Polarization ratio} = \frac{3\cos^2\xi_{a,b} + \sin^2\xi_{a,b}}{\cos^2\xi_{a,b} + 2\sin^2\xi_{a,b}}. \qquad (1)$$

Because 355 nm photoselection distributes the transition dipole moments of the *cis* band of the bleached RHO according to $\cos^2\theta$ relative to the photolysis polarization axis, Eq. 1 can be used with the polarization ratio observed for the 498-nm band to show that the angle between the *cis* and 498-nm band transition dipoles is 38°. A table of values for this function was used similarly to determine the angles of the transition dipole moments of the long wavelength bands of all the species observed, both with respect to the 498-nm band (477 nm excitation) and *cis* band (355 nm excitation) transition dipoles of RHO. These are given in Table 2. The uncertainties were estimated by propagating the uncertainties given in Table 1 and rounding up to the next larger degree.

It is clear from Table 2 that the BSI transition dipole lies in the plane defined by the 498-nm and *cis* band transition dipoles. This is a consequence of the fact that the sum of the angles between the BSI transition dipole and the two RHO transition dipoles, $\xi_{BSI,cis} + \xi_{BSI,498}$, is equal to the angle between the two transition dipoles

TABLE 2 Transition dipole moment angles

	498 nm band	*cis* band
	degrees	*degrees*
BATHO	8 ± 2	42 ± 1
BSI	11 ± 2	27 ± 1
LUMI	12 ± 1	35 ± 1

themselves, $\xi_{cis,498}$. The fact that the sums $\xi_{LUMI,498} + \xi_{LUMI,cis}$ and $\xi_{BATHO,498} + \xi_{BATHO,cis}$ are greater than $\xi_{cis,498}$ indicates that the LUMI and BATHO transition dipole moments cross the *cis*-498 plane. Defining the polar angle around the 498-band transition dipole and measuring from the *cis* band transition dipole as shown in Fig. 4, the polar angles are $\pm(68° \pm 5°)$ for LUMI and $\pm(120° \pm 20°)$ for BATHO. Because either positive or negative values for either angle are consistent with our measurements, we cannot determine on which side of the plane these transition dipoles lie based on our experiments alone.

Simulation of low temperature photochemistry

Bathorhodopsin was originally assumed to be a single species (Yoshizawa and Kito, 1958) . Later experiments (Sasaki et al., 1980) to further characterize bathorhodopsin which had been trapped at liquid nitrogen temperatures suggested that two separate bathorhodopsin species, batho$_1$ and batho$_2$, were present under those conditions. The implication was that a photon could produce either batho$_1$ or batho$_2$ from RHO and that each of these bathorhodopsin species separately decayed to subsequent products, i.e., a parallel decay model. Because results from room temperature photolysis measurements suggest that a single form of bathorhodopsin is produced after light absorption (Hug et al., 1990), we conducted a simulation of the low-temperature experiments where two forms of bathorhodopsin were observed to better understand the nature of the batho$_1$ and batho$_2$ seen there. As shown below, this analysis was aided by the polarization information described above.

In the low-temperature experiments (Sasaki et al., 1980) RHO was photolyzed at 77 K using 437 nm light to produce bathorhodopsin stable at that temperature. Spectra were taken at intervals as the photolysis progressed and irradiation was continued until the absorbance at 480 nm became constant, signifying that a photostationary state had been reached. The progress of photolysis was measured by

$$P_{480} = \mathrm{Log}\left(\frac{A(0) - A(t)}{A(\infty) - A(0)}\right), \qquad (2)$$

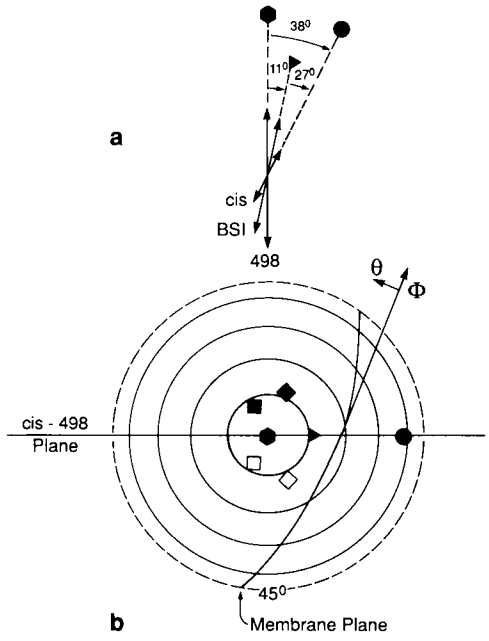

FIGURE 4 Diagram of the transition dipole moments of rhodopsin and its early photolysis intermediates derived from the sequential model with equilibrium between BATHO and BSI. (*a*) View of the transition dipole moments which lie in the *cis*-498 plane of the retinal molecule. Lengths of the lines are proportional to the oscillator strength of the bands. Symbols on the line extensions are used to designate the transition dipole orientation in the polar plot shown in *b*. (*b*) Polar plot of the transition dipole moments of rhodopsin and its early photolysis intermediates. The system shown in *a* is now viewed from the top and the transition dipoles are extended to the surface of a unit sphere. Rhodopsin's transition dipole defines the pole and circles are drawn at 10° increments out to 45° from the pole. Squares show possible positions of the bathorhodopsin transition dipole, diamonds show possible positions of the lumirhodopsin transition dipole. By analogy with the results from frog rhodopsin studies, it is likely that either the open or solid symbols correspond to the actual orientations of the BATHO and LUMI transition dipoles. Extending the analogy allows the placement of the direction of the membrane plane cutting the unit sphere as shown. The θ and ϕ directions shown correspond to those used by Michel-Villaz et al. (1982). From the discussion in the text it can be seen that motion which increases θ red shifts the absorbance, whereas decreasing θ blue shifts the bands.

with $A(t)$ being the absorbance of the sample at 480 nm after photolysis duration t. When P_{480} was plotted vs. t, a straight line was obtained which indicated that RHO was a homogeneous material. Further evidence for this conclusion came from the observation of a single isosbestic point in the spectra taken at successive times during the photolysis.

Once this steady state condition was established at 77 K the trapped bathorhodopsin was then itself subjected to photolysis using light with wavelengths >650 nm. Spectra were again recorded at intervals and the progress of

photolysis was monitored using a quantity P_{540} analogous to P_{480}, but defined using the absorbance of the sample at 540 nm instead of 480 nm. During this photolysis the isosbestic points between successive spectra shifted a total of ~4 nm; and when P_{540} was plotted vs. t, a curved line resulted. These observations were interpreted to mean that two distinct forms of bathorhodopsin were present.

One possible explanation of the multiple forms of bathorhodopsin observed at 77 K is that the forms arise from different orientational distributions of the bathorhodopsin transition dipole moments. Whereas most photoselection experiments involve linearly polarized light, there is photoselection even for beams of unpolarized light because transition dipole moments lying along the light propagation direction are photolyzed much more slowly than those perpendicular to the propagation direction. We thus conducted a simulation to determine whether the weak photoselection by the unpolarized photolysis beam could account for the observations at 77 K.

The simulation was performed using a Monte Carlo method taking a group of 15,000 RHO molecules with random orientations. The effect of a small amount of unpolarized light at 432 nm[1] was then computed by using the transition dipole moment parameters and quantum yields shown in the first two lines of Table 3. Successive increments of light were treated analogously except that after the first irradiation some of the molecules were no longer RHO and for these the transition dipole parameters and quantum yields of the appropriate species in the table had to be used. The size of the irradiation steps was increased as time progressed, and no individual step photolyzed >0.5% of the simulated sample. After each irradiation step the absorbance of the sample was calculated to determine the progress of photolysis. For absorbance measurements the monitoring beam was assumed to be unpolarized and to be colinear with the photolysis beam. Absorbance at a range of wavelengths was computed periodically to detect isosbestic shifts. For the photolysis of RHO, a plot of P_{475} (see footnote 1) vs. irradiation time produced a straight line as shown in Fig. 5 *A* and over the range of photolysis shown there, little isosbestic shift was observed (<0.5 nm), consistent with the actual observations at low temperature.

The simulation then continued by computing the change in composition when the mixture of species produced in the first step was irradiated with 650 nm light. Progress of photolysis was computed using P_{535} (see footnote 1) and the simulated spectra were again used to monitor the isosbestic. The result was that shown in Fig. 5 *B*, a pronounced curvature in the plot of P_{535} vs. t. In addition, the isosbestic was observed to shift ~4 nm to the blue during photolysis of the bathorhodopsin mixture, again in good agreement with the low temperature observations.

[1]There is a red shift in the absorbance maxima of visual pigments when they are observed at 77 K. Because we used values appropriate for room temperature in Table 3, we simulated the red shift by using photolysis and monitoring wavelength values blue shifted by 5 nm.

TABLE 3 Parameters in solid-state rhodopsin partial bleaching simulation

	λ_{max}*	$\Delta\lambda$*	ϵ‡	Angle§	Φ_{RHO}‖	Φ_{ISO}‖	Φ_{BATHO}‖
RHO	500	50	40,000	0	0.33	0.0	0.67
RHO	340	100	8,000	40	0.33	0.0	0.67
Isorhodopsin	485	50	44,000	0	0.0	0.8	0.2
Isorhodopsin	340	100	8,000	40	0.0	0.8	0.2
BATHO	535	50	44,000	−10	0.25	0.05	0.7
BATHO	440	70	10,000	−10	0.25	0.05	0.7

*The spectra of the intermediates used in the simulation were represented by sums of Gaussians with the parameters given in the table. ‡Extinction coefficients for the main bands are representative of the values reported in Packer, whereas values tabulated for the subsidiary bands are estimates consistent with reported spectra. §The angles given are those of the transition dipole moment measured relative to the transition dipole moment of the 498-nm band of RHO. ‖The quantum yields, $\Phi_{species}$, are those derived from Hurley et al.(1977) and Suzuki and Callender (1981). They represent the quantum yield of formation of the subscripted species from the initial material denoted in the left column.

Some of the values in Table 3 are necessarily estimates, but the qualitative conclusions of the simulation are principally determined by those parameters that have been measured experimentally. For example, the linearity of RHO photolysis is principally due to three conditions: (*a*) the fact that photolysis involves two bands with substantially different transition dipole moment directions, i.e., involvement of the *cis* band; (*b*) the fact that the transition dipole of the product does not differ greatly from the reactant; (*c*) the high quantum yield for photolysis. Qualitatively, the curvature of the bathorhodopsin photolysis plot is due to the fact that there is no contribution from a *cis* band in the photolysis of bathorhodopsin, and that the small quantum yield of bathorhodopsin photolysis amplifies the curvature. These general conclusions emerged from many runs in which the relevant parameters were varied to determine the sensitivity of the photochemical model.

DISCUSSION

One of our objectives in measuring polarized spectra was to place constraints on the models used to describe the early photolysis intermediates of RHO. As described in the introduction, the three models discussed here are the parallel, simple sequential, and sequential model with a reversible step between BATHO and the second intermediate. The parallel model was not used to fit the polarization data because of the underdetermined nature of the

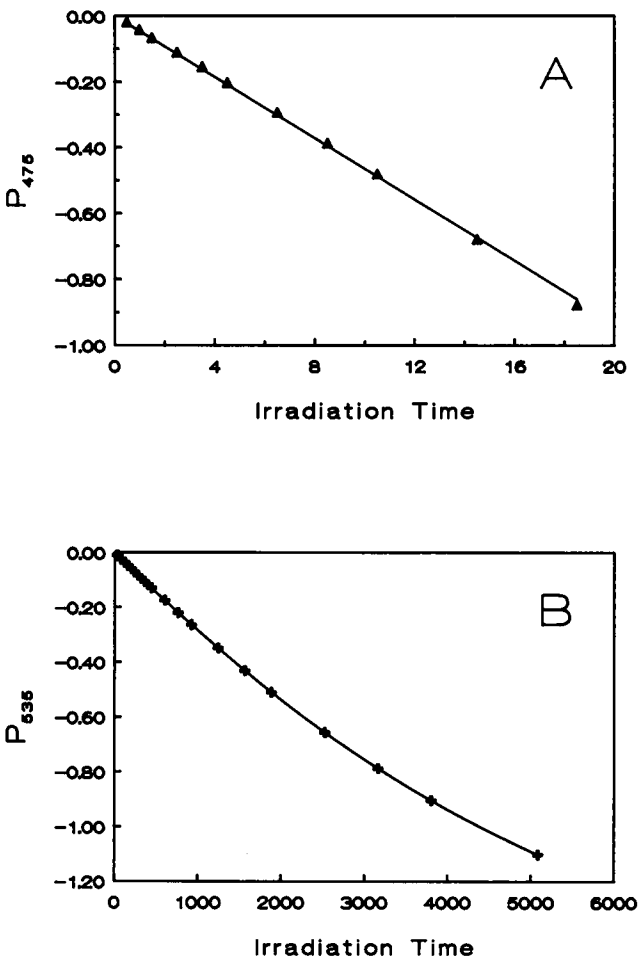

FIGURE 5 Progress of photolysis vs. irradiation time as calculated by the Monte Carlo simulation described in the text. (*A*) Photolysis of a pure rhodopsin sample by 432 nm light monitored by the quantity P_{475}. Actual data are compared to a straight line fit of the data. (*B*) Photolysis of bathorhodopsin, produced as in part *A*, by 650 nm light and monitored by P_{535}. Line through the data is two component fit determined by stripping (i.e., straight line fitting the long time points, then straight line fitting the remaining data points after the long time contribution was subtracted).

spectra for the intermediates involved in that model. Elsewhere we report our attempts using variable excitation wavelengths and powers to perturb the proportions of the two bathos within the parallel model to better define the spectra of its intermediates (Hug et al., 1990). The invariance of the proportions observed along with the results of photolysis experiments on a series of artificial pigments (Einterz et al., 1990), led us to reject the parallel model in favor of sequential models.

The simulation we report here further weakens the case for a parallel model of room temperature photolysis results. One factor in the original proposal of a parallel model at room temperature was the report of two forms of bathorhodopsin at low temperatures. The Monte Carlo simulation shows that the qualitative features of the low temperature experiments can be reproduced using a model of the sequential type. Even quantitatively, the agreement of the simulation with the low temperature experiments is fairly good, with the calculated ratio of fast and slow rates of BATHO photolysis being 3.7 compared to ~4.0 (read from a graph of the low temperature result, Sasaki et al., 1980). The fractional amplitude of the fast component is calculated to be 0.8 vs. reported values which ranged from 0.25 to 0.6 in the low temperature experiments made under different experimental conditions. A simulation cannot include all the factors present in an actual experiment, and here two factors were left out which could affect the results. They were the lack of simulation of the opal glass filter behind the sample and the cracks which potentially form in the sample during freezing. Both of these would tend to scatter the actinic beam, reducing the photoselection effects. They were not included in the simulation because it was impossible to quantitate the degree of scattering involved. If they are not important, the results of the simulation agree quite well with the results of the carefully performed low temperature experiments. If the origin of the two forms of bathorhodopsin observed at 77 K is due to different photoselected orientation distributions, these would not lead to multiple kinetic rates in our room temperature experiments and thus not lend support to a parallel model under our conditions.

The simulation shows that when RHO is excited near 430 nm, the observed photoselection effects are reduced because of participation of two differently polarized bands in the photolysis. The nanosecond polarized absorbance measurements described here support the assumptions of the simulation by demonstrating that the *cis* band differs substantially in transition dipole moment direction from the main band. The conclusion that two transition dipole moments participate in the 437 nm excitation of RHO is supported by a previous report (Strackee, 1972). In contrast, for bathorhodopsin the simulation predicts pronounced photoselection effects even for unpolarized light because photolysis around 650 nm only involves one transition dipole. This gives dramatically different photolysis rates to molecules whose transition dipoles differ in orientation.

The sequential model with a reversible step between BATHO and BSI seems to best fit the polarization data, giving constant polarization ratios for the long wavelength absorption bands of all three intermediates (as is the case for RHO). When a sequential model without the reversible step is used to fit the polarization data, the second intermediate does not have a constant polarization ratio, as is shown in Fig. 3 *B*. The reason this occurs is that the spectrum of the second intermediate in this model is

really composed of a mixture of bathorhodopsin contributing on the red edge of the band and the distinct intermediate BSI contributing absorbance on the blue edge. This explains why the polarization ratio for the second intermediate of the simple sequential model, shown in Fig. 3 *B*, tends toward the value for BATHO on the red side. Thus, in addition to the arguments for a reversible step in the sequential model described elsewhere (Hug et al., 1990), the polarization results further support this conclusion.

Previous measurements of the transition dipole directions for the bathorhodopsin and LUMI intermediates were made using frog ROS rather than the bovine pigment studied here (Michel-Villaz et al., 1982; Kawamura et al., 1979). These previous studies further used oriented membranes, resulting in measurement of transition dipole motion relative to the disk membrane plane (and hence relative to the assumed helix axes). Here our data on randomly oriented membrane suspensions most naturally refer motion to the plane defined by the two transition dipoles of RHO that we are exciting. Our measurements which photolyze RHO in the *cis* (β) band of RHO provide new information about the transition dipole moment of that band.

The angle we measure between the transition dipoles of the 498-nm (α) band and the β band of RHO, 38°, is large enough to justify the designation "*cis* band" for the latter, but is considerably smaller than that calculated even for the twisted naked 11-*cis* retinal (Kakitani and Kakitani, 1979). One factor in the protein that may account for a reduction of this angle is the local dielectric anisotropy, which can be expected to be produced by a molecule like retinal in an elongated protein pocket. Another possibility is that the band being photolyzed with 355 nm light in our experiments is the B band which has been observed in polarized 11-*cis*-retinal crystal spectra. The B band is intermediate in polarization between the almost perpendicularly polarized C band and the main long wavelength A band of 11-*cis*-retinal, making an angle similar to that measured here with respect to the A band (Drikos and Rüppel, 1984).

The value we report for the angle between the transition dipoles of the α band of RHO and BATHO, 8 ± 2°, is in reasonable agreement with the value reported previously by Michel-Villaz et al., 11 ± 3°. The similarity in these values implies that the differences between frog and bovine preparations do not greatly affect the transition dipole directions of the intermediates. This conclusion is further supported by the similar results observed for the linear dichroism of the metarhodopsin II intermediates in these species (Chabre and Breton, 1979). If this conclusion is valid, it becomes possible to use data previously reported on the transition dipole moment of the LUMI intermediate of frog RHO to resolve whether the BATHO and LUMI transition dipoles are on the same or opposite sides of the *cis*-498 plane and to locate the membrane plane on the diagram shown in Fig. 4.

In frog ROS, when BATHO is produced the transition dipole moves principally perpendicular to the membrane plane. Further, the LUMI transition dipole is reported to make the same angle with the membrane plane as the RHO transition dipole does, but may have rotated about the normal to the membrane plane by an undetermined amount (Michel-Villaz et al., 1982). These results imply that for our pigment the transition dipoles of BATHO and LUMI both lie on the same side of the *cis*-498 plane, as shown in Fig. 4. If they lay on opposite sides (e.g., using one solid and one open symbol in Fig. 4), they would both lie roughly in a plane with the 498 band transition dipole. This would not allow the motion caused by the RHO to BATHO change to be approximately perpendicular to the motion of the transition dipole in going from RHO to LUMI, as is observed in frog ROS. Locating both transition dipoles on the same side of the *cis*-498 plane (using only solid or open symbols in Fig. 4) allows this condition to be more nearly met. This suggests that the membrane plane roughly bisects the *cis*-498 angle and is inclined as shown in Fig. 4 by ~25° to the *cis*-498 plane so that the motion of the transition dipole in going from RHO to LUMI is parallel to the membrane plane. Further support for this placement is that it agrees well with the condition that the transition dipole of the 498-nm band be 16° out of the membrane plane (Liebman, 1962) and that the dichroism of the *cis* band be equal to that of the 498 band in ROS (Michel-Villaz et al., 1982; Chabre and Breton, 1979).

Clearly the largest change in transition dipole direction takes place in the BATHO to BSI process. This implies that much greater geometrical change (either movement or shape change) of the chromophore takes place at this time compared to the initial change in the RHO to BATHO process. The large spectral shift which occurs in the BATHO to BSI transition is also consistent with this interpretation. Fig. 4 shows that the transition dipole moves nearly into the plane of the membrane as BATHO becomes BSI. One molecular process which could explain these observations and which must be part of any isomerization mechanism is the straightening of the chromophore. The picosecond formation of BATHO has been taken to imply that isomerization takes place with little geometrical change of the retinal chromophore except for the *cis-trans* isomerization of the $C_{11}{=}C_{12}$ double bond. Any relaxed *trans* chromophore will be considerably longer (straighter) than even a distorted *cis* chromophore. We propose that this straightening leads to motion in the pocket which we observe in the transition dipole movement toward the membrane plane. Subsequent relaxation of the pocket (protein) accounts for formation of LUMI

from BSI as proposed earlier for the BSI intermediate observed after photolysis of 5,6-dihydroisorhodopsin (Albeck et al., 1989). The identification of the BSI intermediates in these two pigments is justified by the similarity in their decay rates as well as the similarity in their spectral shifts relative to the respective pigment spectra. The large qualitative difference in the observed time-dependent spectra seems to be due to the equilibrium constant between BATHO and BSI being higher in the 5,6-dihydroisorhodopsin case, resulting in behavior closely resembling the simple sequential mechanism where the back reaction from BSI to BATHO is negligible (Einterz et al., 1990).

An interesting feature of the transition dipole changes we observe is that rotation of the transition dipole in the pocket seems to be correlated with spectral shift. Such an observation could be caused for example by the rotation arising from chromophore motion relative to a charge near the middle of the retinal as has been recently discussed (Palings et al., 1989). In that model, increased interaction with a negative charge on the opposite side of the chain from the 9-methyl is responsible for the red shift in bathorhodopsin. This model would imply that the blue shift in BSI is caused by motion in the opposite direction, i.e., toward the 9-methyl. Such a model could easily account for the blue shifted spectra of the 11-*cis*-9-demethyl-retinal based pigment (λ_{max} = 463 nm; Kropf et al., 1973) because the absence of the 9-methyl would move the equilibrium position of the chromophore in that direction. If this blue shift is caused by the fact that the 9-demethyl chromophore is already shifted inside the pocket in the blue direction, the model implies that the shift to the blue may be much smaller in these pigments when BSI (if it is blue shifted at all) is formed. Furthermore, when the LUMI state is reached, the absence of the 9-methyl may allow larger movement in the red direction within the pocket (assuming that the C_7–C_{10} region of the chain flips over as has been proposed in several models), predicting that the LUMI from the 9-demethyl pigments should be even more red shifted than that from normal RHO. Preliminary resonance Raman measurements have been reported (Eyring et al., 1980), indicating that the photolysis intermediates of the 9-demethyl pigments are so different that they defy comparison with the normal RHO photolysis intermediates. This supports the idea we propose that the chromophore position is strongly perturbed by the absence of the methyl group. We propose to resolve these questions by making appropriate time-resolved optical density measurements on a 9-demethyl pigment.

The authors would like to acknowledge the fundamental contributions made by previous workers in this field.

This research was supported by a grant from the National Institutes of Health (EY00983).

Received for publication 5 June 1989 and in final form 14 August 1989.

REFERENCES

Albeck, A., N. Friedman, M. Ottolenghi, M. Sheves, C. M. Einterz, S. J. Hug, J. W. Lewis, and D. S. Kliger. 1989. Photolysis intermediates of the artificial visual pigment *cis*-5,6-dihydro-isorhodopsin. *Biophys. J.* 55:233–241.

Chabre, M., and J. Breton. 1979. The orientation of the chromophore of vertebrate rhodopsin in the "meta" intermediate states and the reversibility of the meta II–meta III transition. *Vision Res.* 1:1005–1018.

Cone, R. A. 1972. Rotational diffusion of rhodopsin in the visual receptor membrane. *Nat. New Biol.* 236:39–43.

Drikos, G., and H. Rüppel. 1984. Polarized UV-absorption spectra of retinal isomers-II. On the assignment of the low and high energy absorbance bands. *Photochem. Photobiol.* 40:93–104.

Einterz, C. M., J. W. Lewis, and D. S. Kliger. 1987. Spectral and kinetic evidence for the existence of two forms of bathorhodopsin. *Proc. Natl. Acad. Sci. USA.* 84:3699–3703.

Einterz, C. M., S. J. Hug, J. W. Lewis, and D. S. Kliger. 1990. Early photolysis intermediates of the artificial visual pigment 13-demethyl rhodopsin. *Biochemistry.* In press.

Eyring, G., B. Curry, R. Mathies, R. Fransen, I. Palings, and J. Lugtenburg. 1980. Interpretation of the resonance Raman spectrum of bathorhodopsin based on visual pigment analogues. *Biochemistry.* 19:2410–2418.

Hug, S. J., J. W. Lewis, C. M. Einterz, T. E. Thorgeirsson, and D. S. Kliger. 1990. Nanosecond photolysis of rhodopsin: evidence for a new, blue shifted intermediate. *Biochemistry.* In press.

Hurley, J. B., T. G. Ebrey, B. Honig, and M. Ottolenghi. 1977. Temperature and wavelength effects on the photochemistry of rhodopsin, isorhodopsin, bacteriorhodopsin and their photoproducts. *Nature (Lond.).* 270:540–542.

Kakitani, T., and H. Kakitani. 1979. Molecular mechanism for the initial process of visual excitation. III. Theoretical studies of optical spectra and conformations of chromophores in visual pigments. Their analogues and intermediates based on the torsion model. *Biophys. Struct. Mech.* 5:55–73.

Kawamura, S., F. Tokunaga, T. Yoshizawa, A. Sarai, and T. Kakitani. 1979. Orientational changes of the transition dipole moment of retinal chromophore on the disk membrane due to the conversion of rhodopsin to bathorhodopsin and to isorhodopsin. *Vision Res.* 19:879–884.

Kropf, A., B. P. Whittenberger, S. P. Goff, and A. S. Waggoner. 1973. The spectral properties of some visual pigment analogs. *Exp. Eye Res.* 17:591–606.

Lewis, J. W., J. S. Winterle, M. A. Powers, D. S. Kliger, and E. A. Dratz. 1981. Kinetics of rhodopsin intermediates in retinal rod disk membranes. I. Temperature dependence of lumirhodopsin and meta-rhodopsin I kinetics. *Photochem. Photobiol.* 34:375–384.

Lewis, J. W., J. L. Miller, J. Mendel-Hartrig, L. E. Schaechter, D. S. Kliger, and E. A. Dratz. 1984. Sensitive light scattering probe of enzymatic processes in retinal rod photoreceptor membranes. *Proc. Natl. Acad. Sci. USA.* 81:743–747.

Lewis, J. W., J. Warner, C. M. Einterz, and D. S. Kliger. 1987. Noise reduction in laser photolysis studies of photolabile samples using an optical multichannel analyzer. *Rev. Sci. Instrum.* 58:945–949.

Liebman, P. A. 1962. *In situ* microspectrophotometric studies on the pigments of single retinal rods. *Biophys. J.* 2:161–178.

Michel-Villaz, M., C. Roche, and M. Chabre. 1982. Orientational changes of the absorbing dipole of retinal upon the conversion of rhodopsin to bathorhodopsin, lumirhodopsin and isorhodopsin. *Biophys. J.* 37:603–616.

Neer, E. J., and D. E. Clapham. 1988. Roles of G-protein in transmembrane signalling. *Nature (Lond.).* 333:129–134.

Packer, L., editor. 1982. Biomembranes. I. Visual pigments and purple membranes. *Methods Enzymol.* 81 (*Suppl.*).

Palings, I., E. M. M. van den Berg, J. Lugtenburg, and R. A. Mathies. 1989. Complete assignment of the hydrogen out-of-plane wagging vibrations of bathorhodopsin: chromophore structure and energy storage in the primary photoproduct of vision. *Biochemistry.* 28:1498–1507.

Sasaki, N., F. Tokunaga, and T. Yoshizawa. 1980. The formation of two forms of bathorhodopsin and their optical properties. *Photochem. Photobiol.* 32:433–441.

Stewart, J. G., B. N. Baker, and T. P. Williams. 1977. Evidence for conformeric states of rhodopsin. *Biophys. Struct. Mech.* 3:19–29.

Strackee, L. 1972. Photodichroism of rhodopsin solutions at −196°C. *Vision Res.* 15:253–268.

Suzuki, T., and R. H. Callender. 1981. Primary photochemistry and photoisomerization of retinal at 77°K in cattle and squid rhodopsins. *Biophys. J.* 34:261–265.

Yoshizawa, T., and Y. Kito. 1958. Chemistry of the rhodopsin cycle. *Nature (Lond.).* 189:1604–1605.